Renormalization of the chemical potential due to multiphonon effects at the surface of metals*

Ma Lei(马 磊)[a)b)†], Kang Guang-Zhen(康广振)[a)], and Li Jun(李 俊)[a)]

[a)] National Laboratory of Solid State Microstructures and Department of Physics, Nanjing University, Nanjing 210093, China
[b)] Department of Optics and Electronic Engineering, Zaozhuang University, Zaozhuang 277160, China

(Received 6 March 2012; revised manuscript received 16 April 2012)

We study the relation between renormalization of the chemical potential due to multiphonon effects at the surface of Be(0001) and doping by solving the strong-coupling self-consistent equations of a two-dimensional (2D) electron–phonon interaction system. We present the quasiparticle dispersions and inverse lifetimes of a 2D electron system interacting with Einstein phonons under the different dopings (corresponding to chemical potentials). We find that the effect of electron–phonon interaction on electron structure is strongest at the half filling, but it has no effect on the chemical potential. However, the chemical potential shows distinct renormalization effects away from half filling due to the electron–phonon interaction.

Keywords: kink structure, electron–phonon coupling, renormalization of chemical potential

PACS: 73.20.At, 71.38.–k, 71.10.Ay, 79.60.Bm **DOI:** 10.1088/1674-1056/21/10/107301

1. Introduction

For a long time, the electron–phonon coupling at metal surfaces has attracted much attention due to its fundamental importance in visualizing the basic concepts of many-body theory by photoemission spectroscopy[1,2] and scanning tunneling microscopy.[3] Thorough experimental and theoretical studies of the surface electron states of noble metals have been done. All of these works[4,5] explored the important role of surface phonons in the decay rate of these states. High-resolution photoemission spectra (PES) of the Be(0001) surface states near the Fermi level showed an abrupt change[6] in the dispersion and lifetime of surface state quasiparticles around a critical energy (related to the characteristic phonon frequency). Similar behavior has also been found in high-temperature oxide superconductors,[7−11] other unconventional superconductors,[12,13] and graphene.[14−16] It was suggested that the many-body effects due to electron–phonon interactions may be the cause of this kink structure. All of these would verify a long-time theoretical prediction by Engelsberg and Schrieffer.[17] In their work, the electron–phonon self-energy with the Einstein mode ($w_{\rm ph}$) phonon was obtained under a standard second-order perturbation treatment. But all kinds of features that have been obtained from it are not in agreement with what have been experimentally measured on Be(0001). Then it has been suggested that one needs to use at least the standard result of electron–phonon self-energy with a Debye phonon spectrum to explain the kink structures. The multiphonon processes with Einstein mode phonon has been considered by Tang *et al.*[18] and Phillips,[19] and the results of multi-phonon self-energy are consistent with the results of experiments on the Be(0001) surface and far smaller than the results of single-phonon self-energy.

In this paper, we study the relations between renormalization of the chemical potential and doping due to multiphonon effects by solving the strong-coupling self-consistent equations of a two-dimensional (2D) electron–phonon interaction system. We find that the effect of electron–phonon interaction on electron structure is strongest at the half filling, but it has no effect on the chemical potential. However, the chemical potential shows distinct renormalization effects away from half filling due to the electron–phonon interaction.

*Project supported by the National Natural Science Foundation of China (Grant No. 10574063).
†Corresponding author. E-mail: leima_1017@163.com
© 2012 Chinese Physical Society and IOP Publishing Ltd

2. Model and calculation method

In this paper, our work is based on Ref. [18], in which the aim is to point out the fact that the simplest Einstein phonon mode can also explain the quasiparticle dynamics in PES data of Be(0001) surface states if multiphonon processes are included. To obtain the quasiparticle dispersion and inverse lifetime of 2D electrons interacting with Einstein phonons, we solve the strong-coupling self-consistent equations of a 2D electron–phonon interaction system numerically. The free surface electron state is simply described by the tight-binding approximation (TBA) $\epsilon_{\boldsymbol{k}} = -2t(\cos((k_x) + \cos(k_y)) - \mu$. To study the multiphonon processes and the renormalization of dispersions at different doping, we set the chemical potentials at $\mu = -0.30, -0.15, 0, 0.15$, and 0.30 respectively.

Following the strong-coupling theory, we start from Dyson equation

$$G^{-1}(\boldsymbol{k}, \mathrm{i}\omega_n) = \mathrm{i}\omega_n\sigma_0 - \epsilon_{\boldsymbol{k}}\sigma_3 - \Sigma(\boldsymbol{k}, \mathrm{i}\omega_n), \quad (1)$$

and the electron–phonon self-energy

$$\Sigma(\boldsymbol{k}, \mathrm{i}\omega_n) = \mathrm{i}\omega_n(1 - Z(\boldsymbol{k}, \mathrm{i}\omega_n))\sigma_0 + \chi(\boldsymbol{k}, \mathrm{i}\omega_n)\sigma_3. \quad (2)$$

Here σ_0 and σ_3 are unit and Pauli matrices, respectively. The reason that we still keep Nambu's 2×2 matrix form for the self-consistent equations is that we want to work out not only the single-particle renormalization function $Z(\boldsymbol{k}, \mathrm{i}\omega_n)$ but also the energy level shifting function $\chi(\boldsymbol{k}, \mathrm{i}\omega_n)$, which is usually ignored. No off-diagonal mean fields (related to the superconducting gap) are assumed in this paper. Based on Migdal's theorem, we will only sum over electron–phonon interaction correction to the electron line in the second-order diagram to infinite orders. Then the electron self-energy is given by

$$\Sigma(\boldsymbol{k}, \mathrm{i}\omega_n) = -\frac{1}{\beta}\sum_{\omega_m}\sum_{\boldsymbol{k}'}|g_{\boldsymbol{k}\boldsymbol{k}'}|^2\sigma_3 G(\boldsymbol{k}, \mathrm{i}\omega_m) \times \sigma_3 D(\boldsymbol{k} - \boldsymbol{k}', \mathrm{i}\omega_n - \mathrm{i}\omega_m), \quad (3)$$

where the phonon propagator of the Einstein mode is simply $D(\boldsymbol{k}, \mathrm{i}\omega_\nu) = 2\omega_{\mathrm{ph}}/[(\mathrm{i}\omega_\nu)^2 - \omega_{\mathrm{ph}}^2]$ with phonon frequency $\omega_{\mathrm{ph}} = 70$ meV. This is the maximum phonon frequency experimentally measured and widely cited as the Debye frequency, and this value approximately equals the value of position where the kink structure in the surface state appears in dispersion. We assume a momentum-independent electron–phonon vertex $|g_{\boldsymbol{k}\boldsymbol{k}'}|^2 = g^2 = 0.05$ eV. This kind of simplification is frequently used in model phonon model analysis such as the Einstein model or Debye model. Thus $Z(\boldsymbol{k}, \mathrm{i}\omega_n) = Z(\mathrm{i}\omega_n)$ and $\chi(\boldsymbol{k}, \mathrm{i}\omega_n) = \chi(\mathrm{i}\omega_n)$ are both frequency-dependent only. After some standard algebra operations, we obtain the following self-consistent equations

$$Z(\mathrm{i}\omega_n) = 1 + \frac{\mathrm{i}\omega_n}{g^2}\sum_{\boldsymbol{k}}\int_{-\infty}^{+\infty}\frac{\mathrm{d}\omega'}{\pi}K(\mathrm{i}\omega_n, \omega') \times \mathrm{Im}\left[\frac{Z(\mathrm{i}\omega_m)\mathrm{i}\omega_m}{Q(\boldsymbol{k}, \mathrm{i}\omega_m)}\right]_{\mathrm{i}\omega_m = \omega' + \mathrm{i}\eta}, \quad (4)$$

and

$$\chi(\mathrm{i}\omega_n) = -g^2\sum_{\boldsymbol{k}}\int_{-\infty}^{+\infty}\frac{\mathrm{d}\omega'}{\pi}K(\mathrm{i}\omega_n, \omega') \times \mathrm{Im}\left[\frac{\epsilon_{\boldsymbol{k}} + \chi(\mathrm{i}\omega_m)}{Q(\boldsymbol{k}, \mathrm{i}\omega_m)}\right]_{\mathrm{i}\omega_m = \omega' + \mathrm{i}\eta} \quad (5)$$

for $Z(\mathrm{i}\omega_n)$ and $\chi(\mathrm{i}\omega_n)$, where $Q(\boldsymbol{k}, \mathrm{i}\omega_m) = [Z(\mathrm{i}\omega_m)\mathrm{i}\omega_m]^2 - [\epsilon_{\boldsymbol{k}} + \chi(\mathrm{i}\omega_m)]^2$ and

$$K(\mathrm{i}\omega_n, \omega') = \frac{f(-\omega') + n(\omega_{\mathrm{ph}})}{\mathrm{i}\omega_n - \omega' - \omega_{\mathrm{ph}}} + \frac{f(\omega') + n(\omega_{\mathrm{ph}})}{\mathrm{i}\omega_n - \omega' + \omega_{\mathrm{ph}}} \quad (6)$$

with $f(\omega) = 1/(\,\mathrm{e}^{\beta\omega+1})$ and $n(\omega) = 1/(\,\mathrm{e}^{\beta\omega-1})$ being the Fermi and Bose functions, respectively and we set the temperature $T = 1/\beta = 0.012$ K.

The spectral functions of the upmost component of the Nambu Green's function is

$$\begin{aligned} & A(\boldsymbol{k}, \omega) \\ &= -\frac{1}{\pi}\mathrm{Im}\, G_{11}(\boldsymbol{k}, \mathrm{i}\omega_n = \omega + \mathrm{i}\eta) \\ &= -\frac{1}{\pi}\mathrm{Im}\left[\frac{1}{Z(\mathrm{i}\omega_n)\mathrm{i}\omega_n - \epsilon_{\boldsymbol{k}} - \chi(\mathrm{i}\omega_n)}\right]_{\mathrm{i}\omega_n = \omega + \mathrm{i}\eta}. \end{aligned} \quad (7)$$

The quasipaticle spectrum is defined by root of

$$\omega - (\epsilon_{\boldsymbol{k}}^0 - \mu) - \mathrm{Re}\,\Sigma(\omega + \mathrm{i}0^+) = 0, \quad (8)$$

where $\epsilon_{\boldsymbol{k}}^0$ is the free electron $\epsilon_{\boldsymbol{k}}$ when the chemical potential is zero. The Fermi surface is defined by $\omega = 0$ or

$$\epsilon_{\boldsymbol{k}}^0 = \mu - \mathrm{Re}\,\Sigma(\mathrm{i}0^+). \quad (9)$$

It is clear that the Fermi energy in the electron–phonon interacting system will be different from that in the free electron system if $\mathrm{Re}\,\Sigma(\mathrm{i}0^+)$ would not equal zero. So we have

$$\mu_0 = \mu - \mathrm{Re}\,\Sigma(\mathrm{i}0^+), \quad (10)$$

where μ corresponds to the electron occupancy numbers directly. It should also be noted that $\Sigma(\mathrm{i}0+)$ depend on μ.

The electron distribution function is

$$n_{\boldsymbol{k}} = -\int_{-\infty}^{+\infty}\mathrm{d}\omega' A(\boldsymbol{k}, \omega')f(\omega'). \quad (11)$$

3. Results and discussions

Based on these calculations, some results can be obtained. First, in Fig. 1, we present the real part ($\mathrm{Re}\,\Sigma(\omega)$) and image part ($\mathrm{Im}\,\Sigma(\omega)$) of the electron–phonon self-energy with different chemical potentials ($\mu = -0.30$, -0.15, 0, 0.15, and 0.30). As shown in Fig. 1, $\mathrm{Im}\,\Sigma(\omega)$ increases rapidly from its value at ω=0 and forms a peak at about $\omega \approx 80$ meV, and then saturates at value of 100 meV for $\omega < -100$ mev, while $\mathrm{Re}\,\Sigma(\omega)$ rises linearly from a value near zero at $\omega = 0$, peaks near $\omega \approx 80$ meV, and drops back to zero for $\mu = 0$. However, for $\mu \neq 0$, the peaks of $\mathrm{Re}\,\Sigma(\omega)$ have a shift and are not sharper than the peak for $\mu = 0$. A similar situation also happens in $\mathrm{Im}\,\Sigma(\omega)$ as shown in Fig. 1.

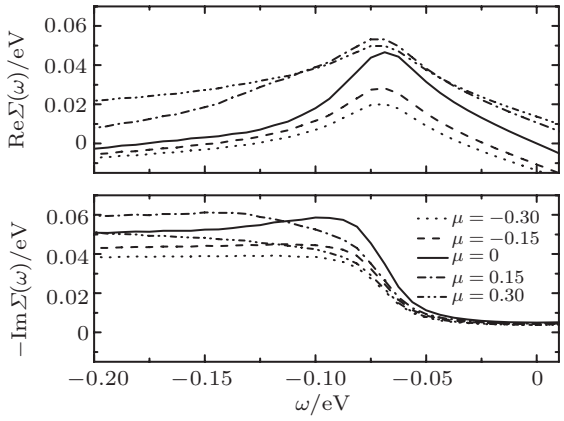


Fig. 1. Real and imaginary parts of the self-energy of the electron–Einstein-phonon interaction for $\mu = -0.30, -0.15, 0, 0.15$, and 0.30.

Second, we obtain the electron spectra by calculating the image part of the self-consistent Green function and present a set of three-dimensional (3D) energy distribution curves (EDC's), which can also be considered as momentum distribution curves (MDC's) if we look at it from a different perspective. Figure 2 is the spectra in a narrow momentum $\boldsymbol{k}$ and ω range near the Fermi level along the Brillouin zone diagonal for $\mu = 0$. The kink structure in the quasiparticle dispersion can be observed clearly, where the two-peak line shape appears in the intermediate region near $E_{\mathrm{F}} - \omega_{\mathrm{ph}}$. So, we can get two branch dispersions.

Next, in Fig. 3, we plot the quasiparticle dispersion obtained by a Lorentzian fit to the MDC's. For the electron–phonon coupling, the description in terms of quasiparticles is only reliable for energies either very close to E_{F} or substantially less than $-\omega_{\mathrm{ph}}$ below E_{F}. From Fig. 3, we can find that the kink is most remarkable for $\mu = 0$. This feature is consist with the change of self-energy for different μ values as shown in Fig. 1. This also proves that electron–phonon interaction is strongest for $\mu = 0$. Moreover, we can find that the dispersions for $\mu \neq 0$ move a little relative to that for $\mu = 0$, which indicates the renormalization of the chemical potential.

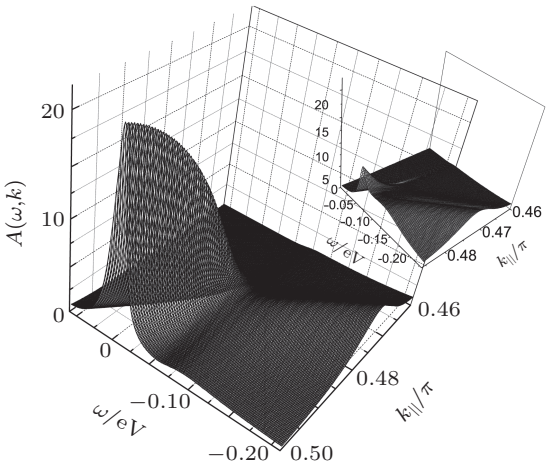


Fig. 2. The spectral functions of the three-dimensional plot with respect to momentum and energy for $\mu = 0$.

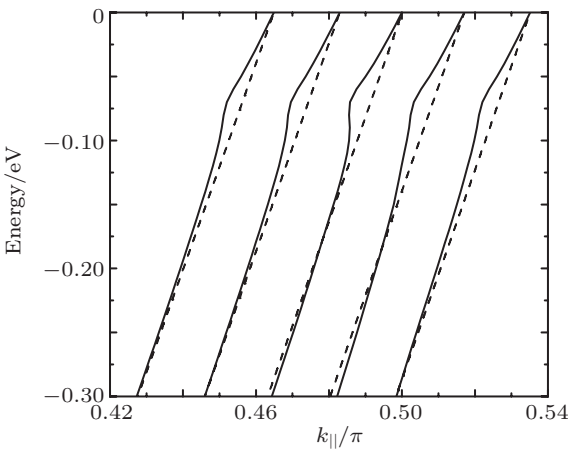


Fig. 3. Quasiparticle dispersions for $\mu = -0.30$, -0.15, 0, 0.15, 0.30 from left to right as plotted by a Lorentzian fit to find the positions of the MDC peak related to the corresponding frequency.

Then we present the relation between electron numbers and chemical potentials with and without considering electron–phonon interaction as shown in Fig. 4. We can observe the renormalization of the chemical potential, as the $\mathrm{Re}\,\Sigma(\omega)$ does not simultaneously vanish at $\omega = 0$. The modification is about 10% at $\mu = 0.30$. So, to get the thermodynamic consistency of the electron number, we must consider the renormalization of μ.

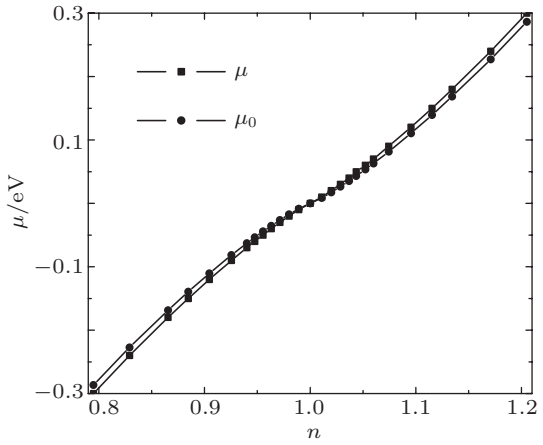


Fig. 4. The renormalization of the chemical potential with electron–phonon interaction. The two curves are the relationship between chemical potential and electron number with (μ_0) and without (μ) electron–phonon interaction respectively.

In Fig. 5, the electron distribution functions at temperature $T = 0.012$ K (near $0\boldsymbol{k}$) are presented. Due to the electron–phonon interaction, they are very like the electron distribution function at a finite temperature.

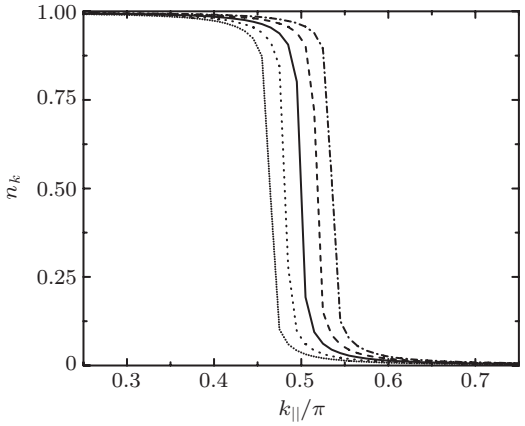


Fig. 5. The electron distribution function curves with electron–phonon interaction correspond to different doping ($\mu = -0.30, -0.15, 0, 0.15, 0.30$) respectively from left to right.

4. Conclusion

In summary, we have solved the strong-coupling self-consistent equations of a 2D electron–phonon interaction system numerically for different doping corresponding to different chemical potentials. We have also obtained self-energy, momentum distribution curves, electron distribution function at a finite temperature, and the relationship between chemical potential and electron numbers. We find that the interaction of electron–phonon for $\mu = 0$ (electrons is half filled in the first Brillouin zone) is strongest and the chemical potential has been renormalized because of electron–phonon interactions. All these results may provide some suggestion for experiments in this respect.

References

[1] Lanzara A, Bogdanov P V, Zhou X J, Kellar S A, Feng D L, Lu E D, Yoshida T, Eisaki H, Fujimori A, Kishio K, Shimoyama J I, Noda T, Uchida S, Hussain Z and Shen Z X 2001 *Nature* **412** 510

[2] Damascelli A, Hussain Z and Shen Z X 2003 *Rev. Mod. Phys.* **75** 473

[3] Kliewer J, Berndt R, Chulkov E V, Silkin V M, Echenique P M and Crampin S 2000 *Science* **288** 1399

[4] Eiguren A, Hellsing B, Reinert F, Nicolay G, Chulkov E V, Silkin V M, Hüfner S and Echenique P M 2002 *Phys. Rev. Lett.* **88** 066805

[5] Hellsing B, Eiguren A and Chulkov E V 2002 *J. Phys.: Condens. Matter* **14** 5959

[6] Hengsberger M M, Purdie D, Segovia P, Garnier M and Baer Y 1999 *Phys. Rev. Lett.* **83** 592

[7] Valla T, Fedorov A V, Johnson P D, Wells B O, Hulbert S L, Li Q, Gu G D and Koshizuka N 1999 *Science* **285** 2110

[8] Valla T, Fedorov A V, Johnson P D, Li Q, Gu G D and Koshizuka N 2000 *Phys. Rev. Lett.* **85** 828

[9] Bogdanov P V, Lanzara A, Kellar S A, Zhou X J, Lu E D, Zheng W J, Gu G, Shimoyama J I, Kishio K, Ikeda H, Yoshizaki R, Hussain Z and Shen Z X 2000 *Phys. Rev. Lett.* **85** 2581

[10] Kaminski A, Randeria M, Campuzano J C, Norman M R, Fretwell H, Mesot J, Sato T, Takahashi T and Kadowaki K 2001 *Phys. Rev. Lett.* **86** 1070

[11] Ren J K, Ren Y F, Tian Y, Yu H F, Zheng D N, Zhao S P and Lin C T 2011 *Chin. Phys.* B **20** 117401

[12] Li Z W, Ma X M, Pang H and Li F K 2012 *Chin. Phys.* B **21** 037104

[13] Ma L, Huang A Q and Li J 2011 *Chin. Phys.* B **21** 047601

[14] Tse W K and Das Sarma S 2007 *Phys. Rev. Lett.* **99** 236802

[15] Calandra M and Mauri F 2007 *Phys. Rev.* B **76** 205411

[16] Bianchi M, Rienks E D L, Lizzit S, Baraldi A, Balog R, Hornekær L and Hofmann P 2010 *Phys. Rev.* B **81** 041403

[17] Engelsberg S and Schrieffer J R 1963 *Phys. Rev.* **131** 993

[18] Tang D M, Li J and Gong C D 2003 *Phys. Rev.* B **67** 235421

[19] Phillips J C 2005 *Phys. Rev.* B **71** 184505